Sains Malaysiana 53(6)(2024): 1405-1419
http://doi.org/10.17576/jsm-2024-5306-14

Molecular Modelling Comparisons, Optical and Band Gap Characterisation of 4-Sulfocalix[4]arene Thin Film

(Perbandingan Pemodelan Molekul, Pencirian Optik dan Jurang Jalur bagi Filem Nipis 4-Sulfokaliks[4]arena)

FARISH ARMANI HAMIDON, FARIDAH LISA SUPIAN*, MAZLINA MAT DARUS, WONG YEONG YI & NUR FARAH NADIA ABD KARIM

Physics Department, Faculty of Science and Mathematics, Universiti Pendidikan Sultan Idris, 35900 Tanjong Malim, Perak, Malaysia

Received: 11 March 2024/Accepted: 8 May 2024

ABSTRACT

The advantageous property of water-soluble calixarenes is their ability to form stable complexes with inorganic guest molecules. Due to these attributes, their application in areas including molecular recognition, sensing, and supramolecular chemistry is extraordinarily alluring. The 4-sulfocalix[4]arene (SC[4]) is a water-soluble molecule and a derivative of the calixarene family that has both aromatic rings and sulfonate groups. The thin films were prepared using a spin-coating technique and characterised by Ultraviolet-Visible Spectroscopy (UV-Vis). By employing the Corey-Pauling-Koltun (CPK) model in conjunction with density functional theory (DFT), the height and diameter of SC[4] were precisely determined by devotedly representing its molecular shape and size. Then, the calixarene thin film's optical properties and light absorption by the thin film were determined using the absorbance graph and Beer-Lambert law equation. The band gap energy of the thin film was determined to be equal to 4.44 eV through the Tauc-plot method. These results substantiate the integration of CPK models validated using DFT for measuring the size of SC[4] molecules and characterising the thin film's optical characteristics. In a nutshell, the implementation of the CPK models was validated with DFT to determine the height and diameter of the SC[4] and the optical characterisation of its thin film was thoroughly determined in this study. The results obtained from this study are not only essential for understanding the properties of SC[4] but also inspire further research for multiple applications such as molecular recognition, adsorption and supramolecular chemistry.

Keywords: Calixarene; Corey-Pauling-Koltun model; spin coating method; ultraviolet-visible spectroscopy

ABSTRAK

Antara manfaat kaliksarena larut air ialah keupayaan dan kemampuannya untuk membentuk kompleks yang stabil dengan molekul tetamu bukan organik. Disebabkan sifat ini, penggunaannya dalam pelbagai bidang termasuk pengecaman molekul, penderiaan dan kimia supramolekul amat menarik perhatian untuk dikaji. 4-sulfokaliks[4] arena (SC[4]) adalah molekul larut air dan terbitan daripada keluarga kaliksarena yang mempunyai cincin aromatik dan kumpulan sulfonat dan selaput nipisnya difabrikasi menggunakan teknik salutan berputar dan dicirikan dengan Spektroskopi Cahaya Tampak-Ultralembayung (UV-Vis). Dengan menggunakan Model Corey-Pauling-Koltun (CPK) dan disahkan bersama dengan teori kefungsian ketumpatan (DFT), ketinggian dan diameter SC[4] ditentukan dengan tepat dalam melambangkan bentuk dan saiz molekulnya secara nyata dan realistik. Kemudian, sifat optik selaput nipis kaliksarena dan penyerapan cahaya oleh selaput nipis tersebut ditentukan menggunakan graf penyerapan dan persamaan Hukum Beer-Lambert. Jurang jalur selaput nipis ditentukan bersamaan dengan 4.44 eV melalui kaedah plot Tauc. Hasil keputusan kajian ini telah mengesahkan integrasi model CPK yang disahkan menggunakan DFT untuk mengukur saiz molekul SC[4] dan mencerap ciri optik selaput nipisnya. Secara ringkasnya, pelaksanaan model CPK disahkan dengan DFT untuk menentukan ketinggian dan diameter SC[4] dan pencirian optik selaput nipisnya telah ditentukan dengan teliti dalam kajian ini. Hasil yang diperoleh daripada kajian ini penting kerana boleh digunakan dalam penyelidikan lanjut untuk pelbagai aplikasi seperti pengecaman molekul, penjerapan dan kimia supramolekul.

Kata kunci: Kaliksarena; model Corey-Pauling-Koltun; spektroskopi cahaya tampak-ultralembayung; teknik salutan berputar

Introduction

4-Sulfocalix[4]arenes (SC[4]) is a water-soluble molecule with numerous advantageous traits in supramolecular chemistry (Atwood et al. 2001; Fahmy et al. 2020; Hu et al. 2015; Shinkai et al. 1984; Tian et al. 2018). It is easily manufactured through direct sulfonation of calixarenes at the upper rim, resulting in high yields. SC[4] is highly attractive for complexing positively charged organic and inorganic guest molecules, which can be stabilised by ionic, cation-π, CH–π, and π–π, hydrophobic, and hydrogen bond interactions (Guo, Wang & Liu 2008). The driving forces for guest inclusion in the cavity are more pronounced in aqueous media than in organic media. The upper rim sulfonate groups and inherent π-electron-rich cavities provide synergistic anchoring sites, resulting in solid binding ability and desirable molecular selectivity towards various organic ions (Chen et al. 2006; Hu et al. 2015; Shinkai et al. 1990; Zhao, Guo & Liu 2013).

Nanomaterials are materials with dimensions between 1 and 100 nm (Cheng 2014; Feldman 2014), which are smaller than the human eye and optical microscopy can resolve. Scientists have created models to study the structure of molecules and particles, which are essential for various scientific fields. Molecular modelling is rapidly evolving and involves creating, representing, and manipulating the three-dimensional structure of chemical and biological molecules. It helps determine physicochemical properties such as visualising the molecular size and shape and understanding molecular interactions in chemical reactions, which are often used in physics, chemistry, and biology. It can aid in molecular design for diverse applications. Molecular-level modelling provides essential information, such as the three-dimensional structure and chemical and physical properties of molecules. It also allows the visualisation of molecular structure complexes and the prediction of new related compounds formed from chemical reactions (Bayda et al. 2020; Bhushan 2017; Nasrollahzadeh et al. 2019; Saleh, Elhaes & Ibrahim 2017; Silakari & Singh 2021).

The molecular modelling or space-filling model is a three-dimensional representation of a molecule that helps to represent the distribution of electrons within atoms realistically. It was developed to represent the relative shape and size of spheres corresponding to the Van der Waal radii (VDW) of atoms based on molecular orbital theory. The Corey-Pauling-Koltun (CPK) model, named after its developers in the 1960s, is used to depict the molecular surface for intermolecular interaction studies. It follows a specific colour scheme, with all colours representing the respective pure chemical elements of the true nature of the atoms. The main advantage of the CPK model is that it shows the entire structure and size of the molecule, which is commonly used in the study of biochemistry for studying the intermolecular interactions between molecules. However, it does not clearly show the chemical bonds between atoms or the internal structure of the molecule (Edelsbrunner & Koehl 2003; Pal 2020, 2019; Xing et al. 2022). The CPK model was built to a scale of 1.25 cm = 0.1 nm =1 Å, allowing for the calculation and measurement of molecular diameter and height (Dillon, Root-Bernstein & Lieder 2006; Gurd 1974).

In addition, density functional theory (DFT) is a widely used computational method in quantum mechanics to describe the electronic structure of molecules and materials (Blinder 2020; Pederson & Baruah 2015). It is based on the electronic density function, which describes the probability of discovering an electron at a specific position in space. Classical molecular mechanics approaches can be used to describe the environment, but quantum mechanical methods are necessary for studying significant electronic structure changes (Corminboeuf, Tran & Weber 2006; De La Lande et al. 2019; Field, Bash & Karplus 1990; Warshel & Karplus 1972; Warshel & Levitt 1976). DFT, developed by Walter Kohn (Haunschild, Barth & French 2019; Kohn 1998; Van Mourik, Bühl & Gaigeot 2014), has been widely used in chemistry and materials science, predicting the properties of small molecules, producing new materials with desired electrical properties, and studying molecular reaction mechanisms and spectroscopic properties (Maurer et al. 2019; Saleh et al. 2023).

Calixarenes are a family of macrocycles with significant conformational flexibility, supporting various guest molecules. However, due to their hydrophobic nature and low water solubility, as aforementioned, its have restricted applications. The synthesis of water-soluble calixarenes via sulfonation, esterification, or etherification, and functionalisation of polar groups has been developed to overcome the problem (Arduini et al. 1984; Ball et al. 2001; Perret, Lazar & Coleman 2006). The significance of water-soluble calixarenes lies in their capacity to overcome the constraints presented by the hydrophobic characteristics and insufficient solubility of ordinary calixarenes. Through solubilising these molecules in water, they extend the range of potential applications in aqueous environments, encompassing biological and environmental circumstances (Budurova et al. 2021; Español & Villamil 2019).

The 4-Sulfocalix[4]arene (SC[4]) is a derivative of the calixarene family, possessing aromatic rings and sulfonate groups shown in Figure 1 (Hu et al. 2015; Shinkai et al. 1984; Tian et al. 2018). SC[4] contains both acidic sulfonate and acidic phenolic groups, with phenolic hydroxyl groups producing intramolecular solid hydrogen bonding. This results in different acid dissociation constants for these OH groups compared to their noncyclic counterparts. Thus, SC[4] exists as multiple ions at neutral pH, requiring sodium counterions for applications and assays. The interaction between SC[4] and alkali metal cations has a lengthy and contentious scientific history (Garcia-Rio, Basílio & Francisco 2020; Millership 2001).

Ultraviolet-Visible Spectroscopy (UV-Vis) is a rapid analytical technique used to characterise molecules by measuring light absorption or transmission (Asahi et al. 2001; Barbosa-García et al. 2007; Owen 1996; Patra & Baek 2014; Rocha et al. 2018; Torres-Rivero et al. 2021). It absorbs a light beam through a sample and detects the light absorbed with a detector at the opposite end. Transmission quantifies the amount of light absorbed

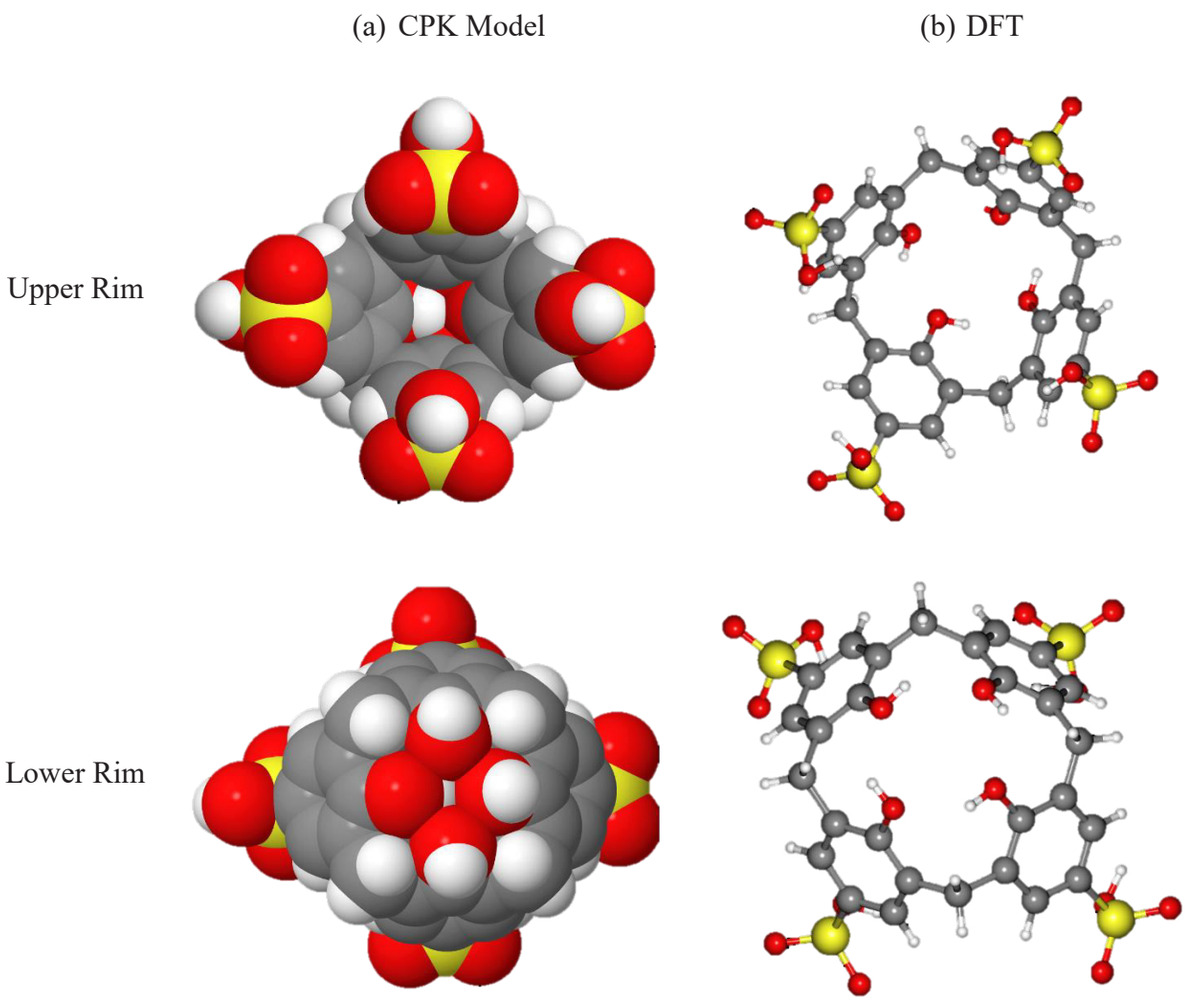

FIGURE 1. Molecular structure of 4-sulfocalix[4]arene from their upper and lower rims view, visualised using (a) the CPK model and (b) Density Functional Theory (DFT)

at various wavelengths, with the significance value max representing the main transition with its maximum intensity. The energy of absorption depends on the configuration of orbital bonds, with simple functional groups absorption at a similar general region (Owen 1996; Rocha et al. 2018; Wypych 2015). When a molecule absorbs UV radiation, electrons are excited from lower to higher energy levels, and the photon's energy must match the energy required by the molecule's electronic structure to absorb the light (Perkampus 1992a, 1992b, 1992c). The Beer-Lambert law states that the absorbance of a solution is linearly proportional to both the concentration of the absorbing material and the path length (Rahimpour et al. 2021; Wypych 2015) shown in Equation (1).

$$A = \log\frac{I_0}{I} = \varepsilon cl \quad (1)$$

A chromophore is a molecular region that absorbs light at a specific wavelength in the ultraviolet and visible regions. It consists of three segments: a potent electron donor segment, a substantial electron acceptor segment, and an π-conjugated bridge (Dinu et al. 2013; Kuball, Höfer & Kiesewalter 2016; Millington 2008; Pentassuglia, Agostino & Tommasi 2018). In the visible and ultraviolet regions, certain bonds and functional groups undergo electronic transitions when absorbing photons. Absorption strength is determined by the probability of transition occurrence and the polarity of an excited state. Nonbonding outer shell electrons (n) contribute the most to visible and ultraviolet light absorption. Molecular molecules also have antibonding orbitals, typically unoccupied, classified as σ* or π*, correlated with excited-state energy levels. Most transitions occur from π or n orbitals to antibonding π* orbitals (Christian, Dasgupta & Schug 2013; Pietrzyk & Frank 1979).

Materials and Methods

Molecular size measurement of SC[4] using CPK model in JSmol software

The study measured and analysed the molecular size of SC[4] using the CPK model in JSmol software, an open-source JavaScript library viewer for 3D chemical structures (Jmol: an open-source Java viewer for chemical structures in 3D 2023; Goodsell & Jenkinson 2018; Hanson et al. 2013; Herráez 2006; Shahzad et al. 2016). The SC[4] molecule was input into JSmol using its International Chemical Identifier (InChI), and the CPK model was applied to the optimised molecule. The JSmol software interface displays the SC[4] molecule.

The molecular size of SC[4] was determined by measuring its upper and lower rim diameters, using the diagonal length between a sulfur molecule and the length between oxygen in the lower rim. The height of SC[4] was indirectly measured by calculating the length of inclined sides and the angle between the tilted side and the horizontal plane. The height was then calculated using trigonometry. The molecular measurement results from JSmol were compared and verified using Density Functional Theory (DFT), which determined the distance between two atoms in a three-dimensional coordinate system using steps similar to the CPK model using the formula in Equation (2) denoted in the coordinate of two atoms in space as illustrated in Figure 2(c) depicting the conducted measurements.

$$d_{2-1} = \sqrt{(x_2 - x_1)^2 + (y_2 - y_1)^2 + (z_2 - z_1)^2} \quad (2)$$

The study compares the means and standard deviations of measurements from the CPK model and DFT to assess the precision and dependability of molecular size prediction of SC[4]. Statistical parameters like means and standard deviations determine data heterogeneity and central tendency. Comparing the standard deviations of the CPK model and DFT measurements demonstrates their coherence and dependability in determining SC[4] molecular size (Kissell & Poserina 2017; Livingston 2004; Loftus 2022; Smith 2015). The mean and standard deviation for distance measurements are calculated using equations adapted from descriptive statistical analysis, which are shown in Equations (3) and (4).

$$\mu = \frac{d_{CPK} + d_{DFT}}{2} \quad (3)$$

$$\sigma = \sqrt{\frac{(d_{CPK} - \mu)^2 + (d_{DFT} - \mu)^2}{2}} \quad (4)$$

Solution preparation

The preparation of an SC[4] solution for thin films was performed in a cleanroom environment (Petty 2005) at Universiti Pendidikan Sultan Idris. The 2.5 mg SC[4] powder was weighed and transferred to a clean vial, then dissolved in 10 mL of deionised water before being agitated or vortexed to ensure even dissolution. The resulting solution had a concentration of 0.25 mg mL^{-1}

and was ready for use (Lim & Supian 2019; Razali et al. 2015). The procedure for preparing the calix[4]arene solution, C[4], was similar but dissolved in chloroform to achieve a concentration of 0.25 mg mL^{-1} due to its solubility in organic solvent. Evaluations between SC[4] and C[4] solutions will be conducted for optical analysis and comparison.

FABRICATION OF THIN FILM USING THE SPIN COATING METHOD

The Elmasonic P70H Ultrasonic cleaning instrument was used for the preparation of the quartz substrate, removing dirt and contaminants from a 25 mm by 25 mm quartz substrate. The process involved soaking the substrate in acetone, treating it with an ultrasonic wave for 10 min, and then bathing it in propanol for similar steps. The substrate was then washed with DI water in between the procedures and dried using a 30 Pa nitrogen gas gun. Subsequently, the substrates were submerged in 1,1,1,3,3,3-hexamethyldisilazane, $C_6H_{19}NSi_2$ (HMDS) vapor for over a day. HMDS was used in the lithography process to enhance the quartz surface to be more hydrophobic, allowing it to react with metals and ceramics to yield hydrophilic trimethyl silanol. This made the surfaces lipophilic, facilitating the adhesion of organic contaminants (Fujimoto, Takeda & Nonaka 2008).

Spin coating was used to uniformly distribute thin layers on flat surfaces using centrifugal force. SC[4] solution was dispensed onto a glass quartz substrate and rotated at 2000 rpm for 15 s to create a single layer. Desired number of layers were repeated for (5, 10, 15, and 20) were achieved, and the substrate was dried using a nitrogen gun after the spin process (Boudrioua, Chakaroun & Fischer 2017; Hassan et al. 1999; Mishra, Bhatt & Bajpai 2019; Supian, Lim & Razali 2017; Yilbas, Al-Sharafi & Ali 2019; Zhang & Hoshino 2018).

CHARACTERISATION OF THE CALIXARENE THIN-FILM USING UV-Vis

This study analysed the optical properties of calixarene thin films using the V570 JASCO spectrophotometer. A solution for both C[4] and SC[4] was generated and its absorbed wavelength fingerprint peaks were compared. The solution synthesised previously was transferred to a cuvette. UV-Vis measurements were conducted within the wavelength range of 200 to 300 nm. The Beer-Lambert law equation was used to determine the molar absorptivity of the solutions for both SC[4] and C[4] from Equations (1). The optical analysis was performed to distinguish between SC[4] and C[4] solutions and evaluate any differences in absorbance outcomes (Böckmann et al. 2015; Lim & Supian 2019; Supian, Lim & Razali 2017).

RESULTS AND DISCUSSION

MOLECULAR MEASUREMENT OF SC[4]

This section analysed the data obtained from the molecular size measurements of SC[4] using the CPK model in JSmol. Firstly, the upper rim of SC[4] was measured, and it was found to be 9.76 Å, slightly different from its parent molecule due to the presence of sulfonate groups in the upper rim. The term 'parent molecule' used in this study refers to the fundamental structure of calixarene, excluding any derivatives or modifications added to its basic form. Next, the lower rim length is measured, and the value is 3.82 Å. Since the lower rim of SC[4] is the same as that of regular calix[4]arene, the length of their lower rims is also similar. The length of the tilting sides of SC[4] was also measured, and it was found to be 5.97 Å, and the angle between the inclined sides and the horizontal plane was found to be 60.1º. The trigonometric formula was used to calculate the height of SC[4], and a value of 5.18 Å was obtained. The longer the tilted side is, the higher the calixarene molecule is, as it can represent conical shapes.

The data were then compared with the experimental data obtained from the CPK Model in JSmol and the theoretical data obtained from DFT calculations to verify the accuracy of the measurements. The diameter of SC[4] obtained from DFT calculations showed that the value of the upper rim diameter is 10.06 Å, and the value of the lower rim is 3.64 Å. Finally, the height of SC[4] obtained from DFT calculations with that obtained from JSmol were compared, and found a slight difference of 0.34 Å, with the value obtained from JSmol being 5.18 Å and that obtained from DFT being 4.84 Å.

Interestingly, the experimental data using the CPK model measurements of the upper and lower rim diameter and height was almost identical to the obtained theoretical data with DFT, demonstrating the precision of distance measurements for this method. This accuracy can be substantiated by calculating the means (μ) and standard deviations (σ) of all the measurements. When conducting a comparison between the CPK Model and the DFT, the degree of dispersion or variability around the means of each dataset can be extrapolated from its standard deviation. As previously mentioned, a low

standard deviation value suggests that the data elements are more closely correlated with the mean, culminating in greater precision and reliability. A comparison between the standard deviations of the CPK model and DFT measurements establishes their consistency and validity in determining the molecular size of SC[4]. In conclusion, the values obtained of SC[4]'s molecular diameters and heights using the CPK Model are consistent with the theoretical values as shown in Figure 2 and Table 1.

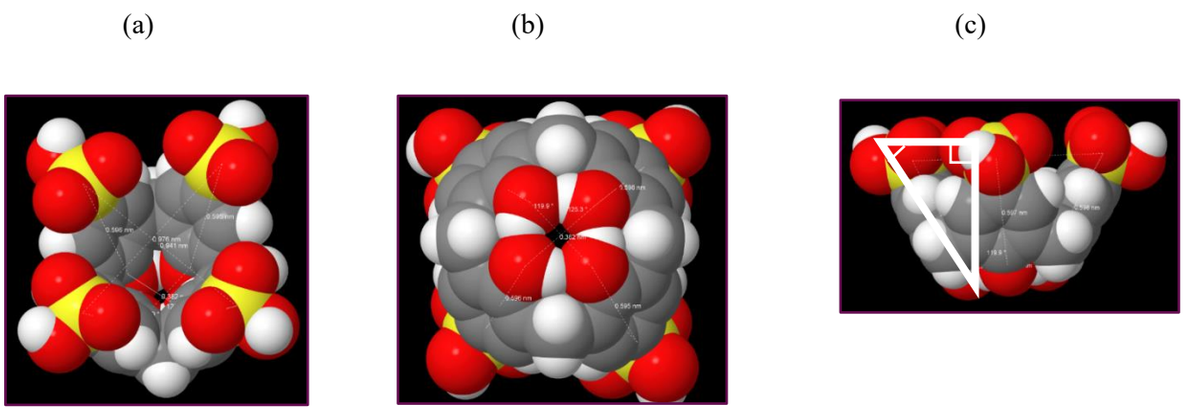

FIGURE 2. Molecular size measurement of SC[4] using CPK Model from JSmol (a) Upper rim diameter, (b) Lower rim diameter, (c) Diagonal length

TABLE 1. [The comparison of the CPK Model with DFT of SC[4]]

	CPK	DFT	Mean (μ)	Standard deviation (σ)
Upper rim Diameter (Å)	9.76	10.06	9.91	0.15
Lower rim Diameter (Å)	3.82	3.64	3.73	0.09
Inclined side length (Å)	5.97	5.89	5.93	0.04
Angle (º)	60.1	55.21	57.66	2.45
Height (Å)	5.18	4.84	5.01	0.17

OPTICAL CHARACTERISATION OF SC[4] SOLUTION AND ITS FILM

Figure 3(a) illustrates the characterisation of the SC[4] and C[4] solutions using UV-visible spectroscopy in the wavelength range of 260 nm to 300 nm. This step is essential for identifying the unique absorption peaks corresponding to the SC[4] solution, which can then be compared to the baseline thin film to ascertain the resiliency of the substrate. Resiliency refers to the usability of the substrate material in fabricating a film onto its surface (Owen 1996). Using the Beer-Lambert Law equation, the data obtained from the UV-visible spectroscopy characterisation were scrutinised to calculate the molar absorption coefficient ε, for both peaks from C[4] and SC[4], as shown in Table 2. The UV absorption of SC[4] solution exhibits absorbance maxima at 277 nm and 283

nm, corresponding to the π-π* transitions. In particular, the absorption spectra of the molecules exhibited two distinct absorption peaks at their maximal absorption, which indicated the presence of aromatic molecules in the SC[4] despite the ring size of the calixarenes (Christian, Dasgupta & Schug 2013; McMurry 2023; Prata, Barata & Pescitelli 2014; Rajavelu & Rajakumar 2018). Therefore, photon absorption results in an electronic transition to an antibonding orbital. Results show the transitions of π-orbitals to antibonding π*-orbitals (π → π*), implying a transition from an excited state to a π* state (Bensenane et al. 2016; Christian, Dasgupta & Schug 2013; Lim & Supian 2019; Pietrzyk & Frank 1979; Wahyuningsih et al. 2017). In contrast, the C[4] solutions exhibit two detectable peaks at 275 nm and 282 nm that are slightly shifted relative to the SC[4] due to the presence of functional sulfonated groups (SO_3H) at the upper rims of SC[4].

The UV-Vis analysis was performed on the SC[4] thin film containing five layers fabricated using the spin coating method on a quartz substrate. The absorbance peak of the thin film occurred at a slightly different wavelength than its solution, as shown in Figure 6 (b). Specifically, there was a blueshift of the peak at 274 nm. However, the SC[4] thin film still exhibited its unique fingerprint absorbance peak. Even if the absorption peaks of the thin film are shifted or expanded relative to those of the solution, this may indicate a change in the structure of the thin film, or perhaps it is undergoing an aggregation process, which can still indicate the stability of the material in solid form, despite the material being deposited as a thin film (Bridges et al. 2016; Fan et al. 2017; Gunawardhana et al. 2019; Li et al. 2017; Lim & Supian 2019).

(a) (b)

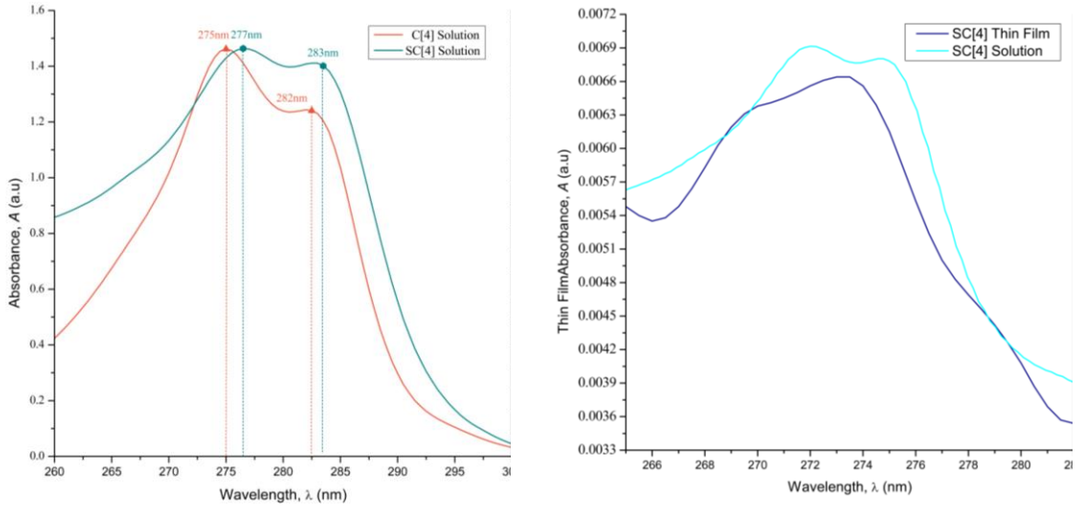

FIGURE 3. (a) The absorption spectra of C[4] and SC[4] solution (b) The absorption spectra of SC[4] solution and its thin film

TABLE 2. [Molar absorptivity of SC[4] and C[4] solution]

	Absorbance peak, λ (nm)	Molar absorptivity, ε ($Lmol^{-1}cm^{-1}$)
C4	275	2482.08
	282	2112.13
SC[4]	277	1241.33
	283	1204.03

Figure 4 shows a molecular-level illustration of how the SC[4] layer may develop on the quartz substrate when deposited during the spin-coating process. The SC[4] molecules have the potential to spread at random across the substrate. Although SC[4] molecules are capable of forming a uniform arrangement, their orientation may exhibit sporadic as they distribute evenly across the surface of the substrate, producing a non-uniform layer.

The results of the absorption spectra of SC[4] solutions obey the Beer-Lambert law (Rahimpour et al. 2021; Wypych 2015), which increases the concentration from 0 μg mL^{-1} to 10 μg mL^{-1}, leads to an increase in absorbance as shown in Figure 5, the UV absorbance of the SC[4] solution across different dilutions that is caused by the amount of chromophore present in a solution that can absorb a specific wavelength of light. One peak was at 283 nm, and another peak was at 277 nm. For every absorbance peak, the molar absorption of SC[4] was determined using the Beer-Lambert Law equation, as shown in Equation 1. Figure 5 shows the absorbance data graph with error bars that indicate the standard deviation around the mean.

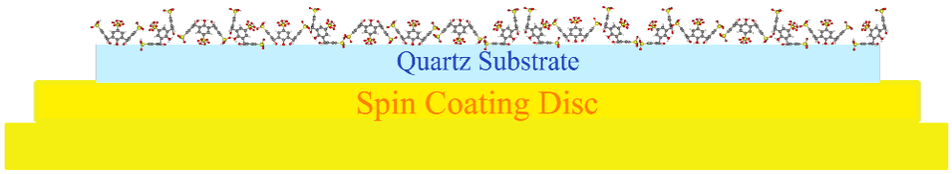

FIGURE 4. Formation of SC[4] films during the spin coating process

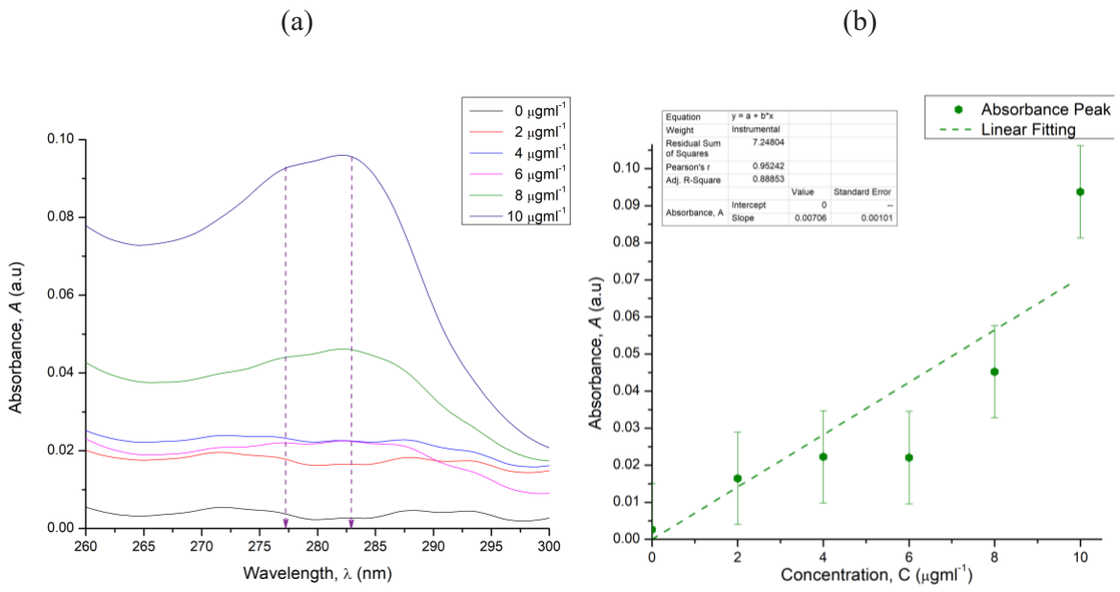

FIGURE 5. (a) Absorption spectra of SC[4] Solutions (b) Absorbance peak as a function of the concentration of SC[4] solution

OPTICAL PROPERTIES OF MULTILAYER THIN FILM OF SC[4]

The spectra of films with different numbers of layers (5, 10, 15, and 20) were obtained using DI water as the solvent, as shown in Figure 6. The absorbance peaks in the spectra exhibited an upward trend in correlation with the number of layers and the film thickness (Acikbas et al. 2017; Özbek et al. 2011). General principles of optical interference may explain this phenomenon. With an increase in the number of layers, the path length of light within the coating also increased, leading to a shift in the phase values of light. These variations in absorbance result from interference effects, either in or out of phase, between the multiple layers of the thin film (Kafle 2020; Ramírez-Santos, Acevedo-Peña & Córdoba 2012).

Furthermore, the findings could potentially be validated by the Beer-Lambert law, which indicates that an increase in the number of film layers, which is equivalent to their thickness, leads to an increase in absorbance because of an extended light path, even if it is not directly related to solution form. In summary, the absorbance of UV-Vis light by the thin film is directly proportional to the number of layers. As the number of layers increases, the film becomes thicker, enhancing the likelihood of light interacting with the material and resulting in more excellent light absorption. Therefore, a higher number of layers in the thin film corresponds to a higher absorbance of UV-Vis light by the film.

BAND GAP ENERGY CALCULATION FOR THE MULTILAYERS SC[4] THIN FILMS

The band gap (Eg) is defined as the difference in energy between the top of the valence band and the bottom of the lowest conduction band, is 0.56eV, nearly half of an empirical band gap value (Motooka & Uda 2015). The optical band gap energy of each multilayer thin film was estimated from the absorption wavelength values (λ) in the UV-Vis spectral data, using the Tauc-plot method from the absorbance graph of UV-Vis by extrapolating the linear part of the graphs to the horizontal Energy, E intercept (Jubu et al. 2022) shown in Figure 7. The calculated energy band gap of the SC[4] thin film for each set was approximately 4.44 eV, as illustrated in Figure 7 and Table 3. The value of the band gap shows that for multilayers SC[4] thin film is an insulator material (Khalifeh 2020).

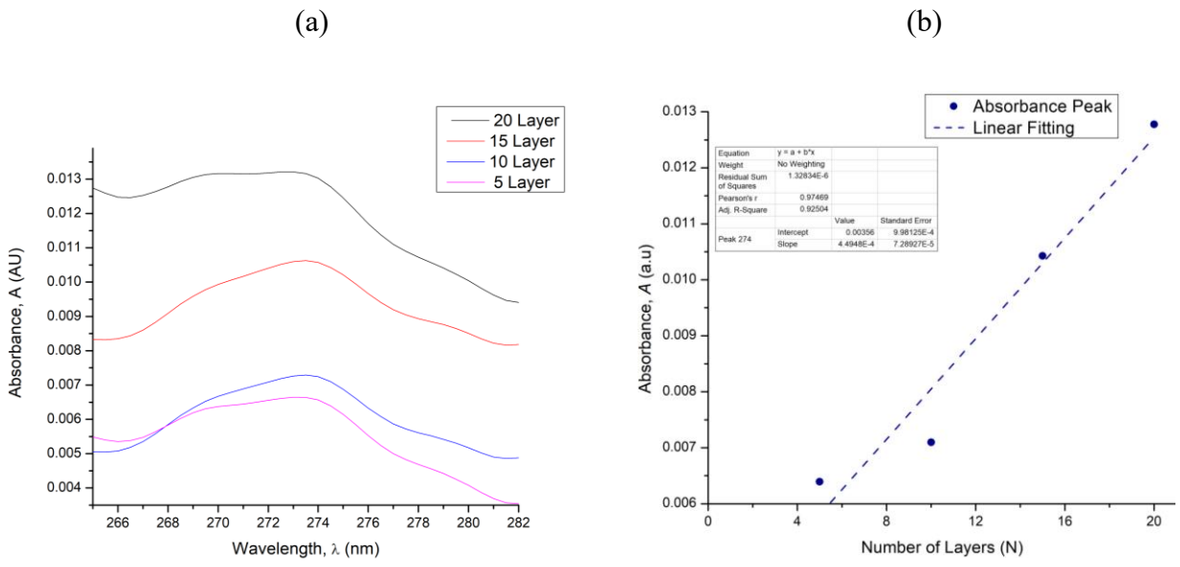

FIGURE 6. (a) The measurement of absorbance for multilayers SC[4] thin film (b) Absorbance peak as a function of the number of layers of SC[4] films

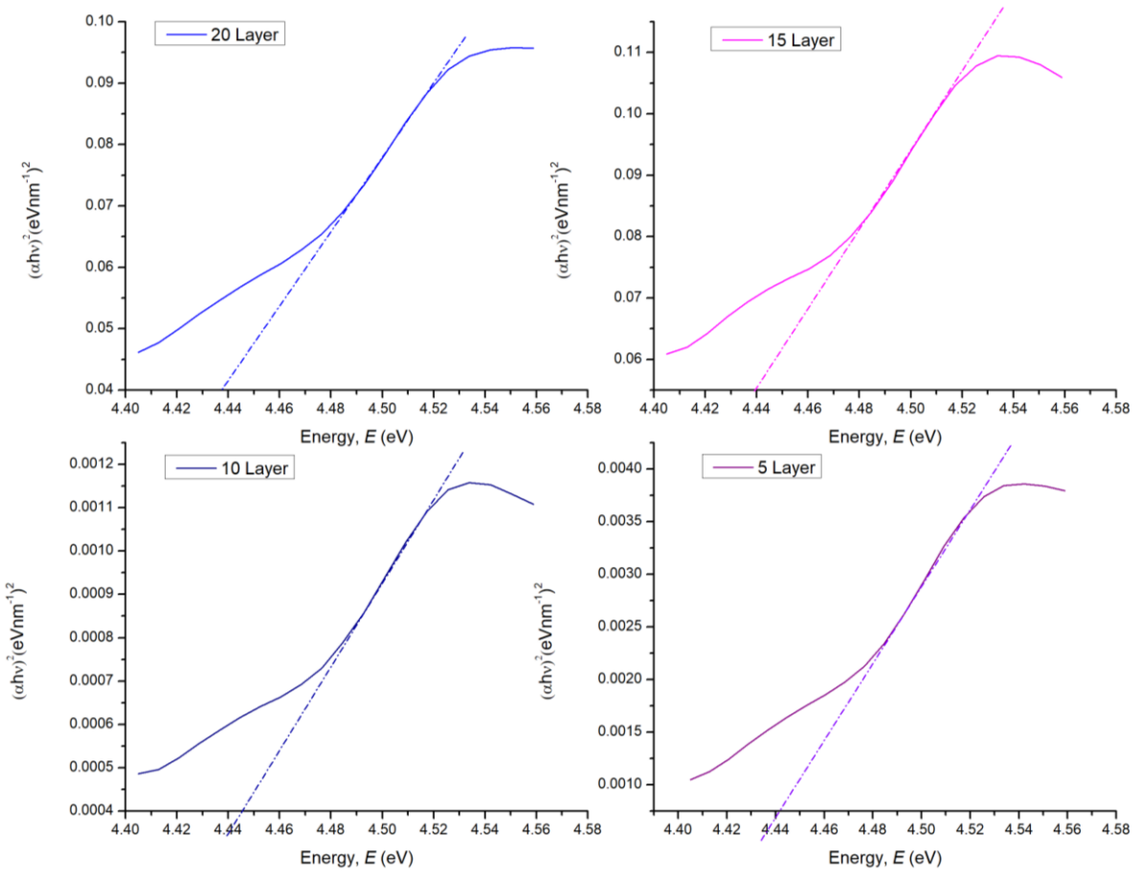

FIGURE 7. Comparison of band gap energy in several multilayered thin films using Tauc-Plot method

TABLE 3. The measurement of the band gap energy of the multilayer thin film

SC[4] thin film (layers)	E_g (eV)
20	4.4373
15	4.4394
10	4.4459
5	4.4490

Conclusions

The main objectives of this study are focused on molecular modelling comparisons with CPK and DFT as well as optically characterising 4-Sulfocalix[4] arene (SC[4]). This includes examining the light absorbance in both films and solutions form, as well as determining the band gap energy. Understanding these optical properties and material behaviour is crucial for applications in analytical chemistry, photovoltaics, and electronics. SC[4] is a water-soluble molecule belonging to the Calixarene family group. CPK, a three-dimensional representation of molecules, is used with density functional theory (DFT) to determine the height and diameter of SC[4]. The CPK model was developed to realistically represent the relative shape and size of spheres corresponding to the Van der Waal radii (VDW) of atoms. Using Ultraviolet-Visible Spectroscopy (UV-Vis), the optical properties and light absorption of the SC[4] thin film were characterised to determine the properties of nanoparticles by measuring light absorption. The optical properties determined consist of molar absorptivity, band gap energies, and light absorption of thin films and solutions. These provide critical understandings of material behaviour that are fundamental for the implementation of analytical chemistry, photovoltaics, and electronics.

Additionally, the Beer-Lambert law of the SC[4] solution was validated, comparing the absorption of the SC[4] and C[4] solutions, and finally, examining the SC[4] solution in relation to its thin films, were all had been conducted with UV-Vis. Using the Tauc-plot method, the band gap energy of the SC[4] thin film was determined, and a value of 4.44 eV was successfully calculated. The results validate the implementation of CPK models verified with DFT for determining the molecular size of SC[4] and effectively characterising the thin film's optical properties. This study's findings can be applied to future research and applications involving SC[4] and calixarenes, such as molecular recognition, sensing, and crystal engineering. In conclusion, the study employed integrated molecular modelling approaches, such as CPK models, Density Functional Theory (DFT) calculations, and experimental optical analysis, to obtain a comprehensive understanding of the molecular structures and optical properties of SC[4]. This approach significantly improved the study's comprehensiveness and accuracy, achieving a thorough comprehension of the properties of SC[4].

acknowledgements

This research was funded by the Sultan Idris Education University (UPSI) through the Ministry of Higher Education Malaysia's Fundamental Research Grants Scheme 2020-0256-103-02 (FRGS/1/2020/STG07/UPSI/02/2). The authors appreciate everyone who contributed recommendations and support to the completion of this study.

References

Acikbas, Y., Bozkurt, S., Halay, E., Capan, R., Guloglu, M.L., Sirit, A. & Erdogan, M. 2017. Fabrication and characterization of calix[4]arene Langmuir–Blodgett thin film for gas sensing applications. *Journal of Inclusion Phenomena and Macrocyclic Chemistry* 89(1-2): 77-84. doi:10.1007/s10847-017-0732-6

Arduini, A., Pochini, A., Reverberi, S. & Ungaro, R. 1984. *p*-t-Butyl-calix[4]arene tetracarboxylic acid. A water soluble calixarene in a cone structure. *Journal of the Chemical Society, Chemical Communications* 15: 981-982 doi:10.1039/C39840000981

Asahi, R., Morikawa, T., Ohwaki, T., Aoki, K. & Taga, Y. 2001. Visible-light photocatalysis in nitrogen-doped titanium oxides. *Science* 293 (5528). doi:10.1126/science.1061051

Atwood, J.L., Barbour, L.J., Hardie, M.J. & Raston, C.L. 2001. Metal sulfonatocalix[4,5]arene complexes: Bi-layers, capsules, spheres, tubular arrays and beyond. *Coordination Chemistry Reviews* 222(1): 3-32. doi:10.1016/S0010-8545(01)00345-9

Ball, V., Winterhalter, M., Perret, F., Esposito, G. & Coleman, A.W. 2001. P-sulfonatocalix[6]arene is an effective coacervator of poly(allylamine hydrochloride). *Chemical Communications* 1(21): 2276-2277. doi:10.1039/b106361h

Barbosa-García, O., Ramos-Ortíz, G., Maldonado, J.L., Pichardo-Molina, J.L., Meneses-Nava, M.A., Landgrave, J.E.A. & Cervantes-Martínez, J. 2007. UV-vis absorption spectroscopy and multivariate analysis as a method to discriminate tequila. *Spectrochimica Acta - Part A: Molecular and Biomolecular Spectroscopy* 66(1): 129-134. doi:10.1016/j.saa.2006.02.033

Bayda, S., Adeel, M., Tuccinardi, T., Cordani, M. & Rizzolio, F. 2020. The history of nanoscience and nanotechnology: From chemical-physical applications to nanomedicine. *Molecules* 25(1): 112. doi:10.3390/molecules25010112

Bensenane, B., Asfari, Z., Platas-Iglesias, C., Esteban-Gómez, D., Djafri, F., Elhabiri, M. & Charbonnière, L.J. 2016. Sulphur-rich functionalized calix[4]arenes for selective complexation of Hg^{2+} over Cu^{2+}, Zn^{2+} and Cd^{2+}. *Dalton Transactions* 45(38): 15211-15224. doi:10.1039/c6dt02628a

Bhushan, B. 2017. *Introduction to Nanotechnology*. 4th ed. Springer Handbooks. doi:10.1007/978-3-662-54357-3_1

Blinder, S.M. 2020. Density functional theory. *Introduction to Quantum Mechanics*. Massachusetts: Academic Press. pp. 235-244. doi:10.1016/B978-0-12-822310-9.00022-7

Böckmann, M., Schemme, T., De Jong, D.H., Denz, C., Heuer, A. & Doltsinis, N.L. 2015. Structure of P3HT crystals, thin films, and solutions by UV/Vis spectral analysis. *Physical Chemistry Chemical Physics* 17(43): 28616-28625. doi:10.1039/c5cp03665h

Boudrioua, A., Chakaroun, M. & Fischer, A. 2017. Organic light-emitting diodes. *An Introduction to Organic Lasers*. ISTE Press - Elsevier. pp. 49-93.

Bridges, C.R., Ford, M.J., Popere, B.C., Bazan, G.C. & Segalman, R.A. 2016. Formation and structure of lyotropic liquid crystalline mesophases in donor-acceptor semiconducting polymers. *Macromolecules* 49(19): 7220-7229. doi:10.1021/acs.macromol.6b01650

Budurova, D., Momekova, D., Momekov, G., Shestakova, P., Penchev, H. & Rangelov, S. 2021. PEG-modified tert-octylcalix[8]arenes as drug delivery nanocarriers of silibinin. *Pharmaceutics* 13(12): 2025. doi:10.3390/pharmaceutics13122025

Chen, F., Li, X., Hihath, J., Huang, Z. & Tao, N. 2006. Effect of anchoring groups on single-molecule conductance: Comparative study of thiol-, amine-, and carboxylic-acid-terminated molecules. *Journal of the American Chemical Society* 128(49): 15874-15881. doi:10.1021/ja065864k

Cheng, X. 2014. Nanostructures: Fabrication and applications. In *Nanolithography: The Art of Fabricating Nanoelectronic and Nanophotonic Devices and Systems*, edited by Feldman, M. Cambridge: Woodhead Publishing. pp. 348-375.

Christian, G.D., Dasgupta, P.K. & Schug, K.A. 2013. *Analytical Chemistry*. 7th ed. John Wiley & Sons Inc.

Corminboeuf, C., Tran, F. & Weber, J. 2006. The role of density functional theory in chemistry: Some historical landmarks and applications to zeolites. *Journal of Molecular Structure: THEOCHEM* 762(1-3): 1-7. doi:10.1016/j.theochem.2005.07.036

de La Lande, A., Alvarez-Ibarra, A., Hasnaoui, K., Cailliez, F., Wu, X., Mineva, T., Cuny, J., Calaminici, P., López-Sosa, L., Geudtner, G., Navizet, I., Iriepa, C.G., Salahub, D.R. & Köster, A.M. 2019. Molecular simulations with in-deMon2k QM/MM, a tutorial-review. *Molecules* 24(9): 1653. doi:10.3390/molecules24091653

Dillon, P.F., Root-Bernstein, R.S. & Lieder, C.M. 2006. Molecular shielding of electric field complex dissociation. *Biophysical Journal* 90(4): 1432-1438. doi:10.1529/biophysj.105.071969

Dinu, R., Miller, E., Yu, G., Chen, B., Scarpaci, A., Chen, H. & Pilgrim, C. 2013. High-speed polymer optical modulators. In *Optical Fiber Telecommunications: Components and Subsystems*, Chapter 5, edited by Kaminow, I.P., Li, T. & Willner, A.E. Massachusetts: Academic Press. pp. 175-204.

Edelsbrunner, H. & Koehl, P. 2003. The weighted-volume derivative of a space-filling diagram. *PNAS* 100 (5) 2203-2208. www.pnas.orgcgidoi10.1073pnas.0537830100

Español, E. & Villamil, M. 2019. Calixarenes: Generalities and their role in improving the solubility, biocompatibility, stability, bioavailability, detection, and transport of biomolecules. *Biomolecules* 9(3): 90. doi:10.3390/biom9030090

Fahmy, S.A., Ponte, F., Sicilia, E. & El-Said Azzazy, H.M. 2020. Experimental and computational investigations of carboplatin supramolecular complexes. *ACS Omega* 5(48): 31456-31466. doi:10.1021/acsomega.0c05168

Fan, Q., Su, W., Guo, X., Wang, Y., Chen, J., Ye, C., Zhang, M. & Li, Y. 2017. Side-chain engineering for efficient non-fullerene polymer solar cells based on a wide-bandgap polymer donor. *Journal of Materials Chemistry A* 5(19): 9204-9209. doi:10.1039/c7ta02075a

Feldman, M. 2014. *Nanolithography: The Art of Fabricating Nanoelectronic and Nanophotonic Devices and Systems*. Woodhead Publishing Limited. doi:10.1533/9780857098757

Field, M.J., Bash, P.A. & Karplus, M. 1990. A combined quantum mechanical and molecular mechanical potential for molecular dynamics simulations. *Journal of Computational Chemistry* 11(6): 700-733. doi:10.1002/jcc.540110605

Fujimoto, T., Takeda, K. & Nonaka, T. 2008. Chapter 7. Airborne molecular contamination: Contamination on substrates and the environment in semiconductors and other industries. In *Developments in Surface Contamination and Cleaning*. 2nd ed., edited by Kohli, R. & Mittal, K.L. William Andrew Publishing. pp. 197-329.

Garcia-Rio, L., Basílio, N. & Francisco, V. 2020. Counterion effect on sulfonatocalix[n]arene recognition. *Pure and Applied Chemistry* 92(1): 25-37. doi:10.1515/pac-2019-0305

Goodsell, D.S. & Jenkinson, J. 2018. Molecular illustration in research and education: Past, present, and future. *Journal of Molecular Biology* 430(21): 3969-3981. doi:10.1016/j.jmb.2018.04.043

Gunawardhana, R., Bulumulla, C., Gamage, P.L., Timmerman, A.J., Udamulle, C.M., Biewer, M.C. & Stefan, M.C. 2019. Thieno[3,2- b]pyrrole and benzo[c][1,2,5]thiadiazole donor-acceptor semiconductors for organic field-effect transistors. *ACS Omega* 4(22): 19676-19682. doi:10.1021/acsomega.9b02274

Guo, D.S., Wang, K. & Liu, Y. 2008. Selective binding behaviors of *p*-sulfonatocalixarenes in aqueous solution. *Journal of Inclusion Phenomena and Macrocyclic Chemistry* 62: 1-21. doi:10.1007/s10847-008-9452-2

Gurd, F.R.N. 1974. The use of Corey-Pauling-Koltun space-filling models in teaching. *Biochemical Education* 2(2): 27-29. doi:10.1016/0307-4412(74)90008-9

Hanson, R.M., Prilusky, J., Zhou, R., Nakane, T. & Sussman, J.L. 2013. JSmol and the next-generation web-based representation of 3D molecular structure as applied to proteopedia. *Israel Journal of Chemistry* 53(3-4): 207-216. doi:10.1002/ijch.201300024

Hassan, A.K., Nabok, A.V., Ray, A.K., Lucke, A., Smith, K., Stirling, C.J.M. & Davis, F. 1999. Thin films of calix-4-resorcinarene deposited by spin coating and langmuir-blodgett techniques: Determination of film parameters by surface plasmon resonance. *Materials Science and Engineering: C* 8-9: 251-255.

Haunschild, R., Barth, A. & French, B. 2019. A comprehensive analysis of the history of DFT based on the bibliometric method RPYS. *Journal of Cheminformatics* 11(1): 72. doi:10.1186/s13321-019-0395-y

Herráez, A. 2006. Biomolecules in the computer: Jmol to the rescue. *Biochemistry and Molecular Biology Education* 34(4): 255-261. doi:10.1002/bmb.2006.494034042644

Hu, X.Y., Peng, S., Guo, D.S., Ding, F. & Liu, Y. 2015. Molecular recognition of amphiphilic *p*-sulfonatocalix[4]arene with organic ammoniums. *Supramolecular Chemistry* 27(5-6): 336-345. doi:10.1080/10610278.2014.967242

Jmol: An open-source Java viewer for chemical structures in 3D. 2023. 'Jmol'. Accessed May 12. http://www.jmol.org/

Jubu, P.R., Obaseki, O.S., Nathan-Abutu, A., Yam, F.K., Yusof, Y. & Ochang, M.B. 2022. Dispensability of the conventional Tauc's plot for accurate bandgap determination from UV–Vis optical diffuse reflectance data. *Results in Optics* 9: 100273. doi:10.1016/j.rio.2022.100273

Kafle, B.P. 2020. Introduction to nanomaterials and application of UV–Visible spectroscopy for their characterization. *Chemical Analysis and Material Characterization by Spectrophotometry*. Elsevier. pp. 147-198. doi:10.1016/b978-0-12-814866-2.00006-3

Khalifeh, S. 2020. Optimization of electrical, electronic and optical properties of organic electronic structures. *Polymers in Organic Electronics*. ChemTec Publishing. pp. 185-202. doi:10.1016/B978-1-927885-67-3.50009-2

Kissell, R. & Poserina, J. 2017. Advanced math and statistics. *Optimal Sports Math, Statistics, and Fantasy*. Elsevier. pp. 103-135. doi:10.1016/B978-0-12-805163-4.00004-9

Kohn, W. 1998. Nobel lecture: Electronic structure of matter-wave functions and density functionals*. *Reviews of Modern Physics* 71: 1253-1266. doi:10.1103/revmodphys.71.1253

Kuball, H.G., Höfer, T. & Kiesewalter, S. 2016. Chiroptical spectroscopy, general theory. In *Encyclopedia of Spectroscopy and Spectrometry*. 3rd ed., edited by Lindon, J.C., Tranter, G.E. & Koppenaal, D.W. Massachusetts: Academic Press. pp. 217-231. doi:10.1016/B978-0-12-409547-2.04980-5

Li, Z., Weng, K., Chen, A., Sun, X., Wei, D., Yu, M., Huo, L. & Sun, Y. 2017. Benzothiadiazole versus thiophene: Influence of the auxiliary acceptor on the photovoltaic properties of donor–acceptor-based copolymers. *Macromolecular Rapid Communications* 39(2): 1700547. doi:10.1002/marc.201700547

Lim, C.K.D. & Supian, F.L. 2019. Calix[4]arene and calix[8]arene langmuir films: Surface studies, optical and structural characterizations. *International Journal of Innovative Technology and Exploring Engineering* 8(8S): 80-85.

Livingston, E.H. 2004. The mean and standard deviation: What does it all mean? *Journal of Surgical Research* 119(2): 117-123. doi:10.1016/j.jss.2004.02.008

Loftus, S.C. 2022. What is statistics and why is it important? *Basic Statistics with R*: *Reaching Decision with Data*. Massachusetts: Academic Press. pp. 3-6. doi:10.1016/B978-0-12-820788-8.00010-9

Maurer, R.J., Freysoldt, C., Reilly, A.M., Brandenburg, J.G., Hofmann, O.T., Björkman, T., Lebègue, S. & Tkatchenko, A. 2019. Advances in density-functional calculations for materials modeling. *Annual Review of Materials Research* 49(1): 1-30. doi:10.1146/annurev-matsci-070218

McMurry, J. 2023. Benzene and aromaticity. In *Organic Chemistry: A Tenth Edition*. Rice University: OpenStax. https://openstax.org/details/books/organic-chemistry

Millership, J.S. 2001. A preliminary investigation of the solution complexation of 4-sulphonic calix[n]arenes with testosterone. *Journal of Inclusion Phenomena and Macrocyclic Chemistry* 39: 327-331. doi:10.1023/A:1011196217714

Millington, K.R. 2008. Improving the whiteness and photostability of wool. In *Advances in Wool Technology*, edited by Johnson, N.A.G. & Russell, I.M. Woodhead Publishing. pp. 217-247. doi:10.1533/9781845695460.2.217

Mishra, A., Bhatt, N. & Bajpai, A.K. 2019. Nanostructured superhydrophobic coatings for solar panel applications. In *Nanomaterials-Based Coatings: Fundamentals and Applications*, edited by Tri, P.N., Rtimi, S. & Plamondon, C.M.O. Elsevier. pp. 397-424. doi:10.1016/B978-0-12-815884-5.00012-0

Motooka, T. & Uda, T. 2015. Multiscale modeling methods. In *Handbook of Silicon Based MEMS Materials and Technologies*, edited by Lindroos, V., Tilli, M., Lehto, A. & Matooka, T. William Andrew. pp. 241-252. doi:10.1016/B978-0-323-29965-7.00008-7

Nasrollahzadeh, M., Sajadi, S.M., Sajjadi, M. & Issaabadi, Z. 2019. Applications of nanotechnology in daily life. *Interface Science and Technology* 28: 113-143. doi:10.1016/B978-0-12-813586-0.00004-3

Owen, T. 1996. *Fundamentals of Modern UV-Visible Spectroscopy: A Primer*. Hewlett-Packard Company. doi:10.1017/CBO9781107415324.004

Özbek, Z., Çapan, R., Göktaş, H., Şen, S., İnce, F.G., Özel, M.E. & Davis, F. 2011. Optical parameters of calix[4]arene films and their response to volatile organic vapors. *Sensors and Actuators B: Chemical* 158(1): 235-240. doi:10.1016/j.snb.2011.06.011

Pal, S. 2020. Structure analysis and visualization. *Fundamentals of Molecular Structural Biology*. Academic Press. pp. 119-147. Elsevier. doi:10.1016/b978-0-12-814855-6.00006-7

Patra, J.K. & Baek, K.H. 2014. Green nanobiotechnology: Factors affecting synthesis and characterization techniques. *Journal of Nanomaterials* 2014: 417305. doi:10.1155/2014/417305

Pederson, M.R. & Baruah, T. 2015. Self-interaction corrections within the fermi-orbital-based formalism. In *Advances in Atomic, Molecular and Optical Physics*, edited by Arimondo, E., Lin, C.C. & Yelin, S.F. Massachusetts: Academic Press. 64: 153-180. doi:10.1016/BS.AAMOP.2015.06.005

Pentassuglia, S., Agostino, V. & Tommasi, T. 2018. EAB - Electroactive biofilm: A biotechnological resource. In *Encyclopedia of Interfacial Chemistry: Surface Science and Electrochemistry*, edited by Wandelt, K. Elsevier. pp. 110-123. doi:10.1016/B978-0-12-409547-2.13461-4

Perkampus, H-H. 1992a. Analytical applications of UV-Vis spectroscopy. In *UV-VIS Spectroscopy and Its Applications*. Springer Lab Manuals. Springer, Berlin, Heidelberg. doi:10.1007/978-3-642-77477-5_4

Perkampus, Heinz-Helmut. 1992b. Photometers and spectrophotometers. In *UV-VIS Spectroscopy and Its Applications*. Springer Lab Manuals. Springer, Berlin, Heidelberg. doi:10.1007/978-3-642-77477-5_3

Perkampus, Heinz-Helmut. 1992c. *UV-VIS Spectroscopy and Its Applications*. Springer Lab Manuals. Springer, Berlin, Heidelberg. doi:10.1007/978-3-642-77477-5

Perret, F., Lazar, A.N. & Coleman, A.W. 2006. Biochemistry of the *para*-sulfonato-calix [n]arenes. *Chemical Communications* 23: 2425-2438. doi:10.1039/b600720c

Petty, M.C. 2005. Organic thin film architectures: Fabrication and properties. In *Surfaces and Interfaces for Biomaterials*, edited by Vadgama, P. Woodhead Publishing. pp. 60-82. doi:10.1533/9781845690809.1.60

Pietrzyk, D.J. & Frank, C.W. 1979. Qualitative analysis: Ultraviolet, visible, and infrared. *Analytical Chemistry*, 2nd ed. Massachusetts: Academic Press. pp. 410-424. doi:10.1016/B978-0-12-555160-1.50022-8

Prata, J.V., Barata, P.D. & Pescitelli, G. 2014. Inherently chiral calix[4]arenes with planar chirality: Two new entries to the family. *Pure and Applied Chemistry* 86(11): 1819-1828. doi:10.1515/pac-2014-0707

Rahimpour, M.R., Makarem, M.A., Kiani, M.R. & Sedghamiz, M.A. 2021. *Nanofluids for Heat and Mass Transfer*. Elsevier. https://doi.org/10.1016/C2020-0-00358-0.

Rajavelu, K. & Rajakumar, P. 2018. Synthesis, characterization, photophysical and electrochemical properties of triazinooxacalix[2]arenes with bisphenol a motif. *Tetrahedron* 74(22): 2812-2818. doi:10.1016/j.tet.2018.04.064

Ramírez-Santos, Á.A., Acevedo-Peña, P. & Córdoba, E.M. 2012. Enhanced photocatalytic activity of TiO_2 films by modification with polyethylene glycol. *Química Nova* 35(10): 1931-1935. doi:10.1590/S0100-40422012001000008

Razali, A.S., Supian, F.L., Abu Bakar, S., Richardson, T.H. & Azahari, N.A. 2015. The properties of carbon nanotube on novel calixarene thin film. *International Journal of Nanoelectronics and Materials* 8: 39-45.

Rocha, F.S., Gomes, A.J., Lunardi, C.N., Kaliaguine, S. & Patience, G.S. 2018. Experimental methods in chemical engineering: Ultraviolet visible spectroscopy-UV-Vis. *Canadian Journal of Chemical Engineering* 96(12): 2512-2517. doi:10.1002/cjce.23344

Saleh, J., Haider, S., Akhtar, M.S., Saqib, M., Javed, M., Elshahat, S. & Kamal, G.M. 2023. Energy level prediction of organic semiconductors for photodetectors and mining of a photovoltaic database to search for new building units. *Molecules* 28(3): 1240. doi:10.3390/molecules28031240

Saleh, N.A., Elhaes, H. & Ibrahim, M. 2017. Design and development of some viral protease inhibitors by QSAR and molecular modeling studies. In *Viral Proteases and Their Inhibitors*, edited by Gupta, S.P. Massachusetts: Academic Press. pp. 25-58. doi:10.1016/B978-0-12-809712-0.00002-2

Shahzad, F., Sheltami, T.R., Shakshuki, E.M. & Shaikh, O. 2016. A review of latest web tools and libraries for state-of-the-art visualization. *Procedia Computer Science* 98: 100-106. doi:10.1016/j.procs.2016.09.017

Shinkai, S., Araki, K., Matsuda, T., Nishiyama, N., Ikeda, H., Takasu, I. & Iwamoto, M. 1990. NMR and crystallographic studies of a p-sulfonatocalix[4] arene-guest complex. *Journal of the American Chemical Society* 112(25): 9053-9058. doi:10.1021/ja00181a004

Shinkai, S., Mori, S., Tsubaki, T., Sone, T. & Manabe, O. 1984. New water-soluble host molecules derived from calix[6] arene. *Tetrahedron Letters* 25(46): 5315-5318. doi:10.1016/S0040-4039(01)81592-6

Silakari, O. & Singh, P.K. 2021. Fundamentals of molecular modeling. *Concepts and Experimental Protocols of Modelling and Informatics in Drug Design*. Massachusetts: Academic Press. 1-27. doi:10.1016/b978-0-12-820546-4.00001-5

Smith, G. 2015. Descriptive statistics. *Essential Statistics, Regression, and Econometrics*. Massachusetts: Academic Press. pp. 71-98. doi:10.1016/B978-0-12-803459-0.00003-0

Supian, F.L., Lim, D.C.K. & Razali, A.S. 2017. Conductivity comparison of calix[8]arene-MWCNTs through spin coating technique. *Sains Malaysiana* 46(1): 91-96. doi:10.17576/jsm-2017-4601-12

Tian, X., Chen, L.X., Yao, Y.Q., Chen, K., Chen, M.D., Zeng, X. & Tao, Z. 2018. 4-sulfocalix[4]arene/cucurbit[7]uril-based supramolecular assemblies through the outer surface interactions of cucurbit[n]uril. *ACS Omega* 3(6): 6665-6672. doi:10.1021/acsomega.8b00829

Torres-Rivero, K., Bastos-Arrieta, J., Fiol, N. & Florido, A. 2021. Metal and metal oxide nanoparticles: An integrated perspective of the green synthesis methods by natural products and waste valorization: Applications and challenges. *Comprehensive Analytical Chemistry* 94: 433-469. doi:10.1016/bs.coac.2020.12.001

Van Mourik, T., Bühl, M. & Gaigeot, M.P. 2014. Density functional theory across chemistry, physics and biology. *Philosophical Transactions of the Royal Society A: Mathematical, Physical and Engineering Sciences* 372(2011): 20120488. doi:10.1098/rsta.2012.0488

Wahyuningsih, S., Wulandari, L., Wartono, M.W., Munawaroh, H. & Ramelan, A.H. 2017. The effect of pH and color stability of anthocyanin on food colorant. *IOP Conference Series: Materials Science and Engineering* 193: 012047. doi:10.1088/1757-899X/193/1/012047

Warshel, A. & Levitt, M. 1976. Theoretical studies of enzymic reactions: Dielectric, electrostatic and steric stabilization of the carbonium ion in the reaction of lysozyme. *Journal of Molecular Biology* 103(2): 227-249. doi:10.1016/0022-2836(76)90311-9.

Warshel, A. & Karplus, M. 1972. Calculation of ground and excited state potential surfaces of conjugated molecules. I. Formulation and parametrization. *Journal of the American Chemical Society* 94(16): 5612-5625. doi:10.1021/ja00771a014.

Wypych, G. 2015. *Handbook of UV Degradation and Stabilization.* 2nd ed., Chemtech Publishing. doi:10.1016/C2014-0-01351-2

Xing, J., Takeuchi, K., Kamei, K., Nakamuro, T., Harano, K. & Nakamura, E. 2022. Atomic-number (Z)-correlated atomic sizes for deciphering electron microscopic molecular images. *Proceedings of the National Academy of Sciences* 119(14): e2114432119. doi:10.1073/pnas

Yilbas, B.S., Al-Sharafi, A. & Ali, H. 2019. Surfaces for self-cleaning. *Self-Cleaning of Surfaces and Water Droplet Mobility*. Elsevier. pp. 45-98. doi:10.1016/b978-0-12-814776-4.00003-3

Zhang, J.X.J. & Hoshino, K. 2018. Fundamentals of nano/microfabrication and scale effect. *Molecular Sensors and Nanodevices*. 2nd ed. Massachusetts: Academic Press. pp. 43-111. doi:10.1016/b978-0-12-814862-4.00002-8

Zhao, H.X., Guo, D.S. & Liu, Y. 2013. Binding behaviors of *p*-sulfonatocalix[4]arene with gemini guests. *Journal of Physical Chemistry B* 117(6): 1978-1987. doi:10.1021/jp312744d

*Corresponding author; email: faridah.lisa@fsmt.upsi.edu.my